Applied Nanoscience (2019) 9:7–17
https://doi.org/10.1007/s13204-018-0896-4

ORIGINAL ARTICLE

Folate-tagged chitosan-functionalized gold nanoparticles for enhanced delivery of 5-fluorouracil to cancer cells

Jude Akinyelu[1] · **Moganavelli Singh**[1]

Received: 12 January 2018 / Accepted: 13 October 2018 / Published online: 19 October 2018

Abstract

Nanoparticles composed of therapeutic drugs are suggested as a promising approach for improved drug delivery to tumour cells. Herein, we report the synthesis of 5-fluorouracil (5-FU) encapsulated chitosan (C) functionalized gold (G) nanoparticles (CG5-FU-NPs) and a folate (F) linked counterpart (FCG5-FU-NPs) for enhanced anticancer effects with reduced adverse reactions. Ionic complexation was used to accomplish 5-FU–excipient interaction and the drug encapsulation efficiencies of the nanoparticles were determined appropriately. UV–visible spectroscopy, TEM, FTIR and nanoparticle tracking analysis (NTA) were used to determine the physiochemical properties of the NPs. Also, dynamic dialysis method was used to determine the rate of drug release at simulated tumour and physiological pH conditions. Cell viability was investigated by the MTT assay in human breast adenocarcinoma (MCF-7), hepatocellular carcinoma (HepG2) and kidney (HEK293) cells. CG5-FU-NPs and FCG5-FU-NPs presented as spherical nanoparticles with a size range of 31–33 nm, and showed surface plasmon resonance bands (SPR) between 520 and 525 nm, thus confirming the synthesis of G-NPs. FTIR spectroscopy confirmed the presence of chitosan and folate chitosan on the nanoparticles. CG5-FU-NPs and FCG5-FU-NPs were highly stable as suggested by zeta measurements of approximately + 61.9 mV and + 57.9 mV, respectively. The NPs attained a drug encapsulation efficiency of > 70%, and produced a pH dependent release of 5-FU. Furthermore, both NPs exhibited an enhanced tumour-specific cytotoxicity compared to the free drug, with FCG5-FU-NPs showing significant targeted delivery potential to the folate receptor-positive MCF-7 cells. These results suggest that CG5-FU-NPs and FCG5-FU-NPs are promising therapeutic systems for cancer management.

Keywords 5-Fluorouracil · Gold nanoparticles · Chitosan · Folic acid · Cytotoxicity

Introduction

Cancer is known for its uncontrollable proliferation of cells. Normal cells undergo programmed cell death, however, cancer cells are immortal, leading to infinite growth of abnormal cells. The use of nanoparticles (NPs) in chemotherapeutic drug delivery systems has recently gained widespread interest owing to the laudable properties they possess, such as improved permeability and retention, which promotes their cellular uptake and delivery. Interestingly, NPs own a surface that could be functionalized to bind or adsorb, and convey pharmacological agents, which makes them highly suitable carriers (Steichen et al. 2013). Furthermore, NPs protect drugs from systemic degradation, enable sustained drug release, improve bioavailability, reduce possible toxic side effects, and offer appropriate methods for different routes of drug administration (Bertrand et al. 2014). From the array of available NPs, the use of inert metallic particles has recently become popular due to their innate optical features, relative safety and suitable biocompatibility (Dauthal and Mukhopadhyay 2016). Gold nanoparticles (G-NPs) have an extensive range of biomedical applications, which include its use in diagnosis, targeted delivery of drugs, biosensors, and photo-thermal therapy (Nivethaa et al. 2015). However, the agglomeration of G-NPs during reduction of its metal salt poses a major challenge, enforcing the need for their stabilization. Polymers and enzymes have proven to be effective stabilizers of GNPs (Upadhyaya et al. 2015; Singh et al. 2014).

✉ Moganavelli Singh
singhm1@ukzn.ac.za

[1] Non-Viral Gene Delivery Laboratory, Discipline of Biochemistry, University of KwaZulu-Natal, Private Bag X54001, Durban, South Africa

Chitosan (C) is a linear biocompatible polysaccharide that can adequately functionalize and stabilize G-NPs in an aqueous medium. Furthermore, Chitosan has many hydroxyl and amino groups which can serve as binding sites for diverse molecules (Božanić et al. 2010; Pauliukaite et al. 2010). Investigations have shown the control of drug burst release by Chitosan-modified carriers (Kang et al. 2017; Chakravarthi and Robinson 2011), and their increased tumour adhesion and permeability to the tumour site (Lee et al. 2014), hence making them highly suitable in the design of drug delivery systems.

5-FU is an inhibitor of thymidylate synthase that is widely utilized in the treatment of cancer (Parker and Cheng 1990). However, poor bioavailability and off-site toxic effects have constrained its use for cancer treatment. Targeted delivery to specific sites with specifically formulated carriers can enhance the therapeutic potential of 5-FU with reduced adverse effects (Udofot et al. 2015). The folate receptor (FRα) is highly expressed in various human cancers (lungs, neck, throat, renal, liver and breast), and can be targeted for receptor mediated cell internalization of therapeutics. Folate (F) is commonly employed as a folate receptor ligand because they are inexpensive, safe, easy conjugates, retain high folate receptor affinity and exhibit high stability in systematic circulation (Yang et al. 2017; Dhas et al. 2015). Reports have shown that folate-decorated nanocomposites can enhance the intracellular delivery of anti-cancer agents in cells overexpressing the folate receptor (Yang et al. 2017; Samadian et al. 2016). In the present investigation, we aimed at enhancing the cytotoxic efficacy of 5-FU against breast and liver cancer cells, by its encapsulation in GNPs and subsequent functionalization with chitosan and folate-linked chitosan. The prepared nanocomposites were characterized using various analytical techniques, investigated for their drug release potential and their cytotoxicity in the human breast adenocarcinoma cells (MCF-7), hepatocellular carcinoma (HepG2) and embryonic kidney cells (HEK293).

Materials and methods

Gold (III) chloride trihydrate ($HAuCl_4.3H_2O$), chitosan (25 kDa, 75% deacetylated), folic acid, N-cyclohexyl-N′-(2-morpholinoethyl) carbodiimide metho-p-toluenesulfonate (NC), N-Hydroxysuccinimide (NHS) and 5-Fluorouracil (5-FU) were procured from Sigma-Aldrich, St. Louis, USA. 3-[4, 5-dimethylthiazol-2-yl]-2.5-diphenyltetrazolium bromide (MTT), Phosphate buffered saline (PBS), 4-(2-hydroxyethyl)-1-piperazineethanesulfonic acid (HBS), acridine orange (AO), dimethylsufoxide (DMSO), and ethidium bromide were acquired from Merck, Darmstadt, Germany. Fetal bovine serum (FBS) was obtained from Hyclone, Utah, USA. Human breast adenocarcinoma (MCF-7) and hepatocellular carcinoma (HepG2) cells were acquired from Highveld Biologicals, Kelvin, South Africa. Human embryonic kidney cells (HEK293) was sourced from the University of the Witwatersrand (Anti-viral Gene Therapy Unit) South Africa. All cell culture media were procured from Lonza Bio Whittaker, Walkersville, USA. Only Analytical grade reagents were used in this study.

Synthesis of G-NPs

Colloidal G-NPs were synthesized by citrate reduction of Gold (III) chloride trihydrate (Turkevich et al. 1951) and modified (Lazarus and Singh 2016) as reported previously. Trisodium citrate (40 mM) and aqueous colloidal gold solution (3×10^{-2}M) was added to approximately 30 mL of boiling water. The resulting mixture was vigorously stirred for 20 min, resulting in a transition of the yellow coloured solution to a wine red.

Synthesis of CG5-FU-NPs and FCG5-FU-NPs

As illustrated in Fig. 1, 10 mL of G-NP were added to trisodium polyphosphate (TPP) (2×10^{-9}M) in 1 mL of acetic acid solution (1% v/v). A TPP-G-NP solution was then obtained after sonication for 30 min at 21 °C, and stirred for 6 h. The G5-FU was formed by the addition of 500 µL of 5-FU solution (6 mg·mL^{-1}) to 1.5 mL of TPP-G-NP solution, followed by sonication for 30 min at 21 °C and stirring for 6 h. CG-5-FU or FCG5-FU were prepared by dropwise addition of either 0.3% Chitosan or 0.3% Folate-Chitosan (conjugated via carbodiimide /NHS linkage) into the G-5-FU solution at a ratio of 1:4, under sonication at 21 °C for 30 min, and stirred for 6 h. Drug-free carriers were also synthesized without 5-FU, in a similar way. All the synthesized NPs were dialyzed (12 000 MWCO) against Milli-Q water for 12 h and stored at − 10 °C for further use.

Nanoparticle characterisation

UV–Vis spectroscopy (Jasco V-730, Germany) was used to record the absorption spectra of the synthesised NPs. The dry state size, ultrastructural morphology and distribution of synthesized NPs were determined by transmission electron microscopy (TEM) (JEM 1010, Jeol, Tokyo, Japan). The hydrodynamic size and zeta potential of all studied formulations were measured by Smoluchowski modelled doppler anemometry, using nanoparticle tracking analyser (NTA) (NS500, Malvern Instruments, Worcestershire, UK), at 25 °C. To confirm surface functionalization of the G-NPs, attenuated total reflection-Fourier transform infrared

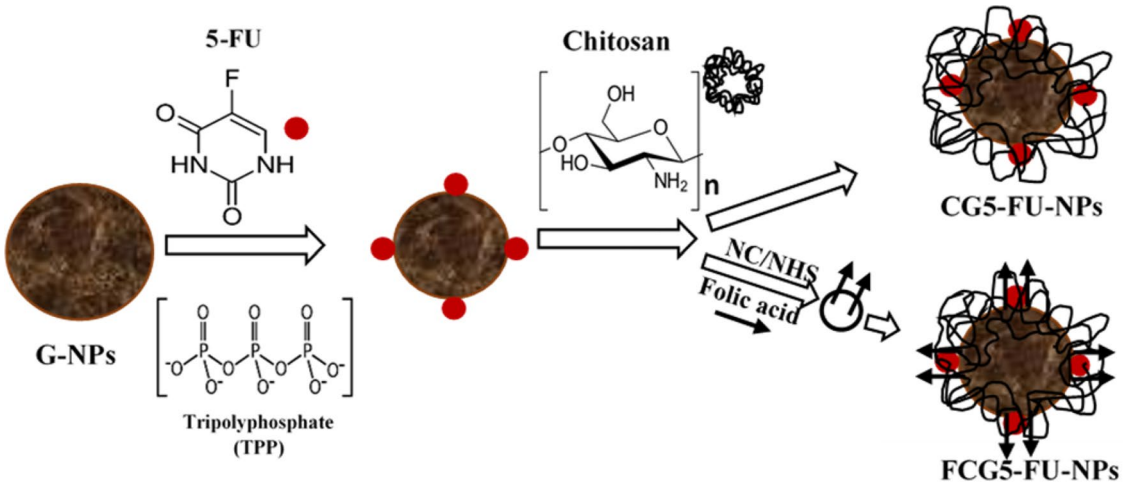

Fig. 1 Schematic illustration depicting the synthesis of CG5-FU-NPs and FCG5-FU-NPs

(ATR-FTIR) spectroscopy (Perkin Elmer Spectrum 100, U.S.A) was performed. The infrared absorption spectra of the NPs were obtained at 25 °C.

Drug encapsulation efficiency (E.E)

To assess the drug encapsulation efficiency, the drug entrapped G-NPs were centrifuged at 20,000 RPM for 30 min at 20 °C. The concentration of 5-FU in the obtained supernatants was measured from a calibration curve by determining the UV absorbance at 266 nm. E.E was estimated using the equation below:

$$\text{E.E}\ (\%) = \left[5-\text{FU}_{\text{total}} - 5-\text{FU}_{\text{supernantant}}\right] / \left[5-\text{FU total}\right] \times 100$$

Drug release studies

Free drug and functionalized drug-coupled G-NP solution (2 ml) were dispensed into dialysis bags (2 kDa MWCO) and suspended inside sealed conical flasks containing phosphate buffer at pH of 5.0 and 7.4. The temperature was maintained under shaking conditions at 37 °C. At specific time intervals, dialysates were withdrawn for analysis and concentration of the drug was estimated from the UV–vis absorbance obtained at 266 nm. The amount of drug released was plotted against time.

Drug release kinetics

To investigate the mechanism of drug release from the nanocomposites, release data were analysed using the following models:

Zero order: $R = k_0 t$ (Sood and Panchagnula 1998).

First order: $R = 1 - e^{-k1} t$ (Sood and Panchagnula 1998).

Korsmeyer-Peppas model: $M_t/M_a = k_5 t^n$ (Ritger and Peppas 1987):where R and M_t/M_a represent fractional drug release at time t, k is the rate constant corresponding to each model, and n denotes the exponent of diffusion. The kinetic models were selected to fit the drug release data and deductions were made from the coefficient of determination (r^2) values. In the Korsmeyer-Peppas model, drug release mechanisms are defined by the release exponent ("n"). An "n" value of 1 signifies zero-order release kinetics (case II transport), $n = 0.5$ signifies Fickian diffusion, $0.5 < n < 1$ corresponds to non-Fickian diffusion (anomalous release), and an "n" value greater than 1 suggests a super case II transport relaxational release (Ofokansi et al. 2007).

Cytotoxicity assay

Cytotoxicity of MCF-7, HepG2, and HEK293 cell lines was investigated using the MTT assay. Cells (2.0×10^4 per well) were seeded in 96-well plates containing growth medium and incubated at 37 °C in a 5% CO_2 incubator for 24 h. In competition experiments, free folate (10 µg) was introduced to cells 30 min prior to the addition of the nanocomposites. Thereafter, the medium was replaced, cells treated with varying concentrations of drug free carriers, free 5-FU and 5-FU encapsulated nanocomposites for 48 h. The spent medium was then removed, and new growth medium containing 10% MTT solution was added and cells incubated for 4 h, followed by removal of the medium/MTT solution and the addition DMSO. Control Cells were incubated at same conditions without the nanocomposites. All assays were done in triplicate. The absorbance at 540 nm was detected in a microplate reader and the percentage cell viability was estimated using the equation below.

% Cell viability = [absorbance of treated cells/absorbance of untreated cells] × 100.

Apoptosis assay

The acridine orange (AO)/ethidium bromide (EB) dual staining method (Maiyo et al. 2016) was used to investigate the effect of the pre-determined half maximal inhibitory concentrations (IC_{50}) of 5-FU encapsulated carriers on cell apoptosis. Briefly, cells (4.5×10^5 per well) were seeded in a 24-well plate and incubated for 24 h. Afterwards, the cells were exposed to the samples and incubated for 24 h at 37 °C. Untreated cells were used as positive controls. Subsequently, cells were rinsed with cold PBS, and dual stain (10 µl) (AO: 0.1 mg.ml^{-1}, EB: 0.1 mg.ml^{-1} in PBS) was added in a reaction time of 5 min. Thereafter, the cells were briefly rinsed with cold PBS and viewed under a fluorescent microscope. The apoptotic index was estimated using the equation below:

Apoptotic index = number of apoptotic cells/number of total cells counted.

Statistics

Statistical analysis was performed using one way ANOVA and Tukey's multiple comparison test (GraphPad Instat 7.3) across all groups. Differences were considered statistically significant at $^{**}p < 0.01$ and $^{*}p < 0.05$.

Results and discussion

Nanoparticle characterization

The formation G-NPs following citrate reduction of $HAuCl_4.3H_2O$, was visually confirmed (Fig. 2), as the reaction mixture turned wine red within 15 min., with further confirmation obtained from the UV–Vis spectroscopic analysis of the G-NP solution (Fig. 2), which displayed maximum absorption in the range of 520–525 nm. Also, CG5-FU-NPs and FCG5-FU-NPs displayed absorption bands at a similar range. Absorption bands in this range is attributable to the surface plasmon excitation of G-NPs (Haiss et al. 2007). A significant decline in the absorption intensity, as well as slight peak shift was shown for CG5-FU-NPs and FCG5-FU-NPs, and may denote a modification in the surface of G-NPs following 5-FU, chitosan and folate adsorption. Nanocomposite formation was corroborated by TEM analysis (Fig. 3), which reveals that majority of the unmodified G-NPs were spherical and uniformly distributed with size range of 31–33 nm (Table.1). Similar distribution, shapes and sizes were obtained for CG5-FU-NPs and FCG5-FU-NPs. This small size is significant, since such nanocarriers of anticancer drugs can easily escape the leaky tumour vasculature and accumulate within the tumour region to exert cytotoxic effects on proliferating cells (Danhier et al. 2010).

The hydrodynamic sizes of the G-NPs, CG5-FU-NPs and FCG5-FU-NPs as determined by NTA (Table 1) were

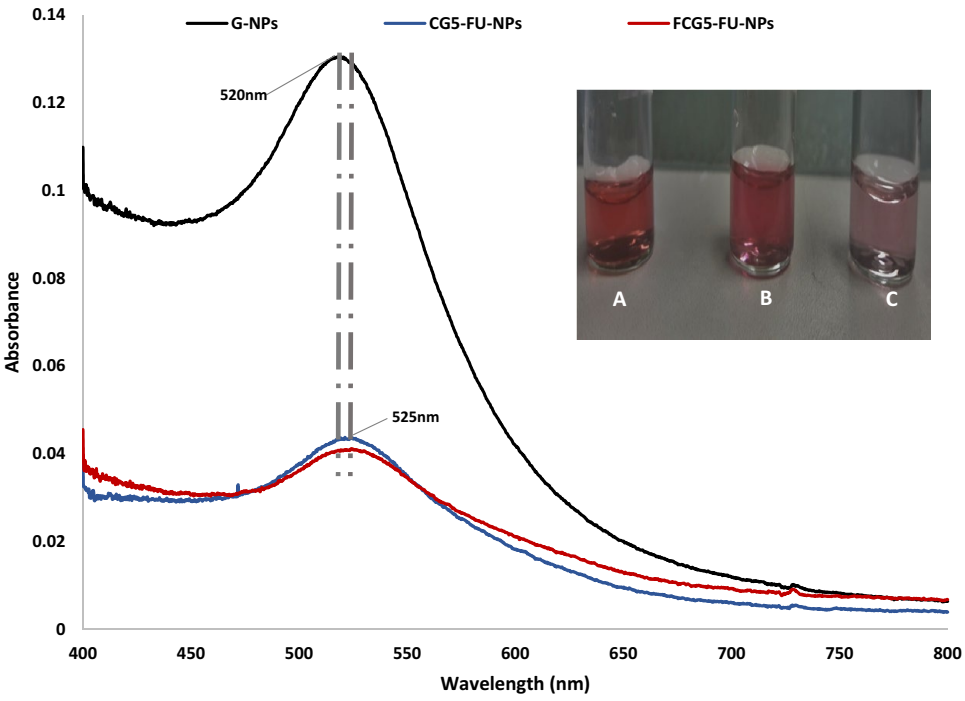

Fig. 2 UV–Vis spectrum of G-NP, CG5-FU-NPs, and FCG5-FU NPs. Inset: Digital photos; [A]: G-NPs, [B]: CG5-FU-NPs, [C]: FCG5-FU NPs

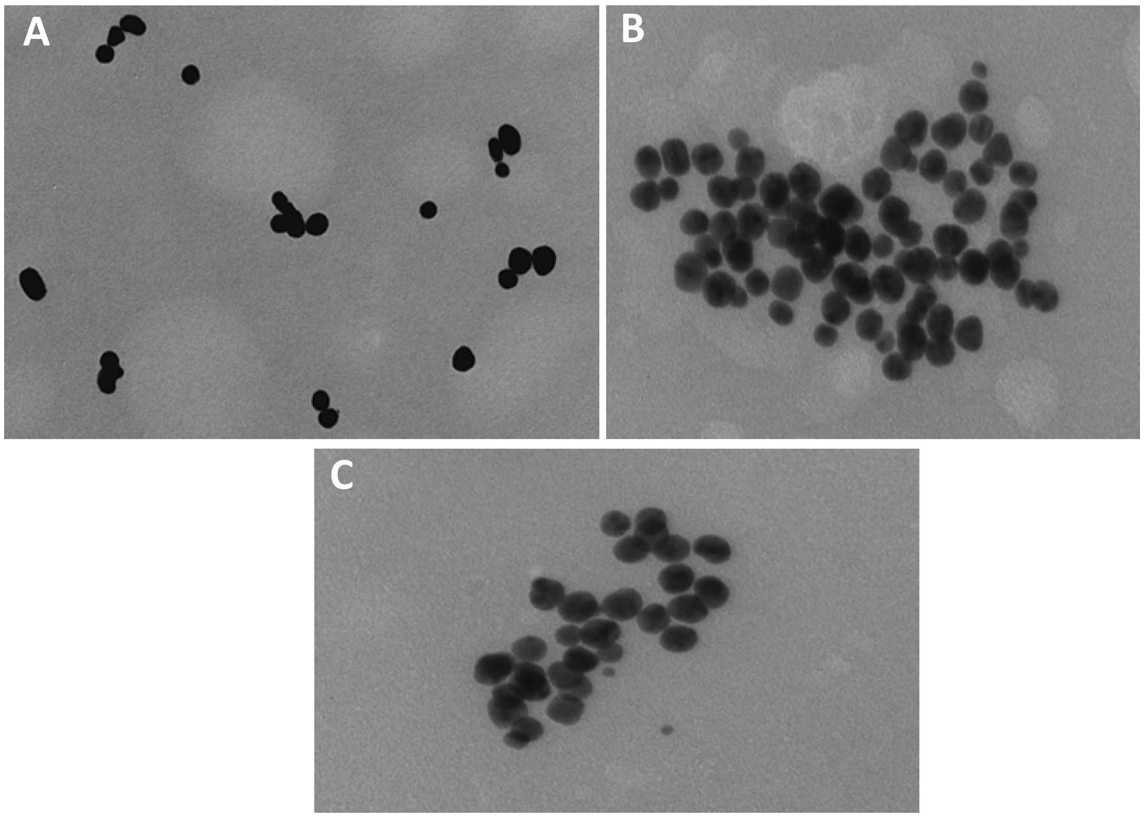

Fig. 3 TEM micrograph images [A] G-NPs, [B] CG5-FU-NPs [C] FCG5-FU-NPs (Scale Bar = 100 nm)

Table 1 TEM size distribution (TSD), hydrodynamic size distribution (HSD), and zeta potential of the synthesized nanocomposites

Nanocomposite	TSD (nm)	HSD (nm)	Zeta potential (mV)
G-NPs	30 ± 1.4	65.9 ± 9.8	− 7.3 ± 1.6
CG5-FU-NPs	31 ± 1.1	126 ± 23.2	61.9 ± 0.1
FCG-5-FU-NPs	33 ± 1.3	149.3 ± 34.2	57.9 ± 1.9

approximately 65.9 nm, 126 nm, and 144 nm, respectively, which were bigger as compared TEM analysis. This may be due to the swelling of the NPs in an aqueous environment, in contrast to TEM which measures the dry state of NP sizes. Furthermore, there may have been some aggregation of the NPs in the aqueous medium contributing to a higher size range.

The zeta potential (ZP) magnitude is an indication of the repulsive forces between particles in suspension, hence, can be used to predict the stability of colloidal aqueous dispersions. CG5-FU-NPs and FCG5-FU-NPs displayed high stability (Table. 1) as denoted by their ZP values of approximately + 57.9 mV and + 61.1 mV, respectively, in contrast to unmodified G-NPs with a ZP value − 7.3 mV. The association of chitosan (C) or folate-chitosan (FC) molecules with 5-FU encapsulated G-NPs is further evidenced by the shift from negative ZP value of unmodified G-NPs to highly positive values of the drug containing nanocomposites. The FCG5-FU-NPs had a lower zeta potential value than its non-folated counterpart, which could be due to the modification of folate by chitosan particles, which causes a reduction in the protonated amino groups of chitosan, leading to the drop in zeta potential. In general, nanocarriers with zeta potential values > + 30 mV or < − 30 mV will tend to be stable (Venkatpurwar et al. 2011), and suitable for drug delivery studies.

The FTIR spectrum (Fig. 4) of chitosan showed a characteristic IR band at ~ 3484 cm^{-1} corresponding to the O-H stretch. The amide group in chitosan is evident by its absorption peak at ~ 1660 cm^{-1}. Similarly, the FTIR spectrum of folic acid showed IR bands at 1480–1700 cm^{-1} indicating C = N bonds, C = O, and the NH_2– group of the pteridine ring in folate. A significant difference is observed between the IR spectra of folate and folate-chitosan. The characteristic amide peak from chitosan at ~ 1680 cm^{-1} shifts to ~ 1640 cm^{-1}, and is overlapped with the newly formed peak due C–N bond, indicating the coupling of folate to chitosan. The IR spectra of 5-FU showed a characteristic C-H stretch in the 2800–2900 cm^{-1} region. The 5-FU bands in ~ 1431–1658 cm^{-1} region were assigned to the C = C and C = N stretching vibrations. The bands at about ~ 1340 cm^{-1} were vibrations of the pyrimidine compound. The absorption

bands at ~ 1178 cm^{-1} and ~ 1256 cm^{-1} were C–O and C–N vibrations, respectively. The characteristic peaks of 5-FU were significantly diminished in the footprint region of the drug, which strongly suggests its encapsulation by chitosan or folate-chitosan functionalized G-NPs. The characteristic bands of chitosan and folate with minor shifts in CG5-FU-NPs and FCG5-FU-NPs, validate the presence folate and folate-chitosan on the designed nano formulations. The assignment of peaks was correlated with earlier studies (Dhar et al. 2008; Wang and Shaw 2014; Salar and Kumar 2016; Yassin et al. 2010).

Encapsulation efficiency

The use of TPP, induced negative charges on the G-NPs and enabled the ionic interaction between the G-NPs and the positively charged 5-FU, which was thereafter functionalized and stabilised with chitosan (C) or folate-chitosan (FC). The encapsulation efficiency of 5-FU by the nanocomposites was estimated based on the amount of 5-FU content in the supernatant after obtaining the nanocomposites from the 5-FU solution. CG5-FU-NPs and FCG5-FU-NPs demonstrated encapsulation efficiencies of 74% and 79%, respectively.

Release studies

Drug release (in vitro) studies were performed at pH 5 and 7.4 to measure the release of 5-FU from the CG5-FU-NPs and FCG5-FU-NPs. These conditions were selected to mimic the acidic tumour micro-environment and physiological environment such as blood with a neutral pH. As represented in Fig. 5, the pH dependent release of 5-FU from the nano formulations was slower compared to free 5-FU. Further, approximately 81% and 69% of drug were cumulatively released from CG5-FU-NPs at pH 5 and 7.4, respectively, after 72 h. The faster release of 5-FU at acidic pH as compared to neutral pH may be due an increased protonation of the repetitive amine groups of chitosan in the acidic release medium. Cationic polymer-derived drug delivery systems are highly soluble in acidic medium, which consequently exposes encapsulated or linked drugs to the release medium (Tan et al. 2017; Carbinatto et al. 2014; Madhusudhan et al. 2014). Also, after 72 h, 90% and 86% of 5-FU were respectively released from FCG5-FU-NPs at pH 5 and 7.4. The remarkable high release rate of 5-FU from the folated nanocomposite at pH 5, and more interestingly at pH 7.4, may be due to increased acidity of the respective release media caused by the presence of folic acid on the targeted nanocomposite. Taken together, it is probable that the acidic environs of tumour cells might elicit the release of 5-FU from the designed delivery vehicles, and importantly, the sustained drug release profile from the vehicles over a long period, would reduce dosing regimens. Earlier studies have also shown the closely similar release profile of 5-FU from cationic modified inorganic nanoparticles at pH 5 and 7.4 (Nivethaa et al. 2015; Safwat et al. 2016).

Kinetic studies

The rate of dissolution of a polymer-based delivery system is influenced by certain variables such as diffusion potential, polymer swelling, polymer erosion and the surrounding environment (Uhrich et al. 1999; Ismail et al. 2017). The in vitro drug release data were fitted into some kinetic models (zero order, first order, and korsmeyer-Peppas) to elucidate the mechanism of drug release. The kinetic evaluation of drug release (Table 2) indicates that the preponderant mechanism of release at acidic and physiological pH was zero order. A claim that was supported by its "*n*" values of between 1.018 and 1.078, which denotes case II release kinetics (Kuksal et al. 2006) (a strong indication of zero order). Interestingly, zero-order model has been reported as an ideal model for sustained drug delivery at a constant rate, which could prolong the pharmacological action of drugs encapsulated by polymer matrix systems (Dash et al. 2010; Maney and Singh 2017). Also, zero–order release can help predict the bioavailability status of drugs, thus improving treatment regimens.

Evaluation of cytotoxicity

The commonly used MTT assay was performed to evaluate the cytotoxic effect of the drug-free carriers, free 5-FU and its encapsulated nanocomposites on the MCF-7, HepG2 and HEK293 cells after 48 h. Our results as represented in Fig. 6a–c, show relatively no cytotoxicity of CG5-FU-NPs and FCG5-FU-NPs in all the investigated cell lines, hence any cytotoxicity observed will not be due to these drug-free carriers. The free 5-FU, CG5-FU-NPs, and FCG5-FU-NPs exhibited a concentration-dependent increase in cytotoxicity

Table 2 Kinetic parameters at pH 5 and 7.4

Nanocomposite	pH	Zero (r^2)	First (r^2)	Korsmeyer-peppas (r^2)	(n)[a]
CG5-FU-NPs	5	0.998	0.850	0.989	1.051
CG5-FU-NPs	7.4	0.990	0.938	0.987	1.018
FCG5-FU-NPs	5	0.999	0.888	0.987	1.078
FCG5-FU-NPs	7.4	0.999	0.946	0.996	1.044

r^2 coefficient

[a]n: Korsmeyer-peppas release exponent

on MCF-7 cells. The half maximal inhibitory (IC_{50}) concentration for of CG5-FU-NPs and FCG5-FU-NPs on MCF-7 cells were 30 µg/mL and 20 µg/mL, respectively, while the free drug at identical concentrations caused < 30% cell death. Furthermore, of CG5-FU-NPs and FCG5-FU-NPs had over 50% cell death in HepG2 cells at a concentration of 40 µg/mL, while free 5-FU exhibited over 70% cell survival at a similar concentration. The enhanced cytotoxicity shown by of CG5-FU-NPs and FCG5-FU-NPs on MCF-7 and HepG2 cells, compared to the free drug, may be attributed to the ability of functionalized G-NPs to evade cellular barriers, thus promoting the controlled release and accumulation of 5-FU in the tumour cells. The cell membrane of cancer cells are highly negative due to increased rate of glycolysis and the associated release of lactic acid (Chen et al. 2016). Equally, positively charged drug delivery systems have strong affinity for negatively charged cell membranes, thus, are more readily internalized. Elsewhere, G-NPs, functionalized with a cationic polymer have been reported to significantly improve the membrane permeability and anticancer effect of 5-FU (Nivethaa et al. 2015). Therefore, it is conceivable that enhancement in the anti-proliferative effect of 5-FU would bring about a decrease in its doing frequency, thereby minimizing the adverse response elicited by constant drug administration. Interestingly, the cytotoxic effect of FCG5-FU-NPs on the MCF-7 cells was significantly higher compared to CG5-FU-NPs at all the investigated concentrations. The presence of folate (F) on the carrier may have promoted particle binding to the folate receptors (FRα) which are expressed on the surface of MCF-7 cells. This interaction may have triggered folate receptor endocytosis, thereby, causing improved internalization of FCG5-FU-NPs by MCF-7 cells. Direct proof of receptor-mediated uptake was shown in a competition assay, using folic acid as the competitor. The results (Fig. 6d), show a significant decrease in the anti-tumour effect of FCG5-FU-NPs on MCF-7 cells pre-incubated with folate. Previous studies have demonstrated an increased cellular uptake of folate conjugated carriers by folate receptor positive cells (Akinyelu and Singh 2018; Devendiran et al. 2016; Song et al. 2013). As there were no folate receptors on the HepG2 cells, FCG5-FU-NPs showed no obvious increase in the cytotoxic effect compared to CG5-FU-NPs. To investigate the cytotoxicity of the nanocomposites towards non-cancer cells, evaluations were performed in HEK293 cells (Fig. 6c). The cell viability of HEK293 at the highest studied concentration of 40 µg/ml of CG5-FU-NPs and FCG5-FU-NPs was > 75%, which implies their relative safety to non-cancer cells. Non-cancer cells are neutrally or slightly positively charged, hence they have no strong affinity for positively charged drug carriers. Therefore, it is evident that the drug-encapsulated nanocomposites exhibit anti-proliferative activity towards cancer cells, while being non-toxic to the surrounding non-cancerous cells.

Table 3 Apoptotic indices of drug encapsulated nanocarriers

Cell lines	CG5-FU-NPs	Apoptotic index FCG5-FU-NPs	FCG-5-FU-NPS (Competition)
MCF-7	0.23	0.56	0.37
HepG2	0.35	0.32	Not determined
HEK-293	0.04	0.03	Not determined

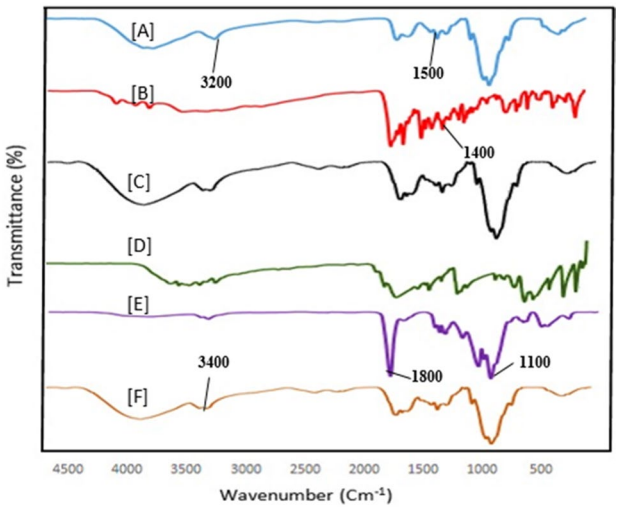

Fig. 4 FTIR spectra of [A] C, [B] F, [C] F-C, [D] 5-FU, [E] CG5-FU-NPs [F] FCG-5-FU-NPs

Apoptosis study

Acridine orange (AO)/ethidium bromide (EB) double staining was employed to investigate if the observed cell death was induced by apoptosis following a 24 h treatment with free 5-FU, CG5-FU-NPs and FCG5-FU-NPs. Viable cells have double-stranded DNA and exhibit green fluorescence upon staining with AO, while non-viable cells are characterised by single-stranded DNA and fluoresce red when stained with AO. Furthermore, living cells have intact DNA and exhibit round green nuclei when stained with EB. Cells with compromised membrane integrity fluoresce red upon EB staining. Early apoptotic (EA) and late apoptotic (LA) cells possess fragmented DNA and exhibit orange-red fluorescence. Apoptotic indices and microscopic cell images are shown in Table 3 and Fig. 7 respectively. All control cells fluoresced green after staining indicating viable states, however, MCF-7 and HepG2 cells which were treated at pre-determined IC_{50} concentrations of CG5-FU-NPs and FCG5-FU-NPs showed some distinctive morphological and biochemical features of apoptosis, such as change in cell shape, cytoplasm shrinkage, and

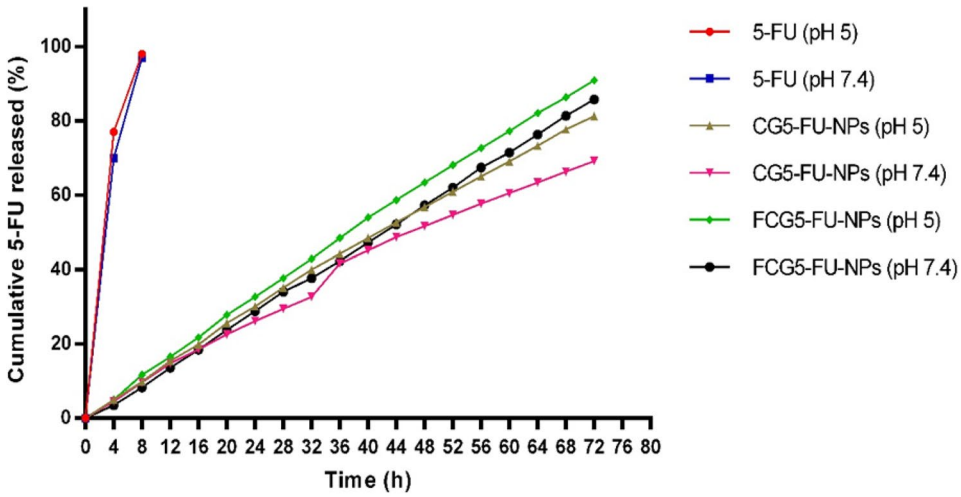

Fig. 5 In vitro release profile of 5-FU encapsulated nanocomposite at pH 5 and 7.4. Data are represented as means ± SD ($n = 3$),

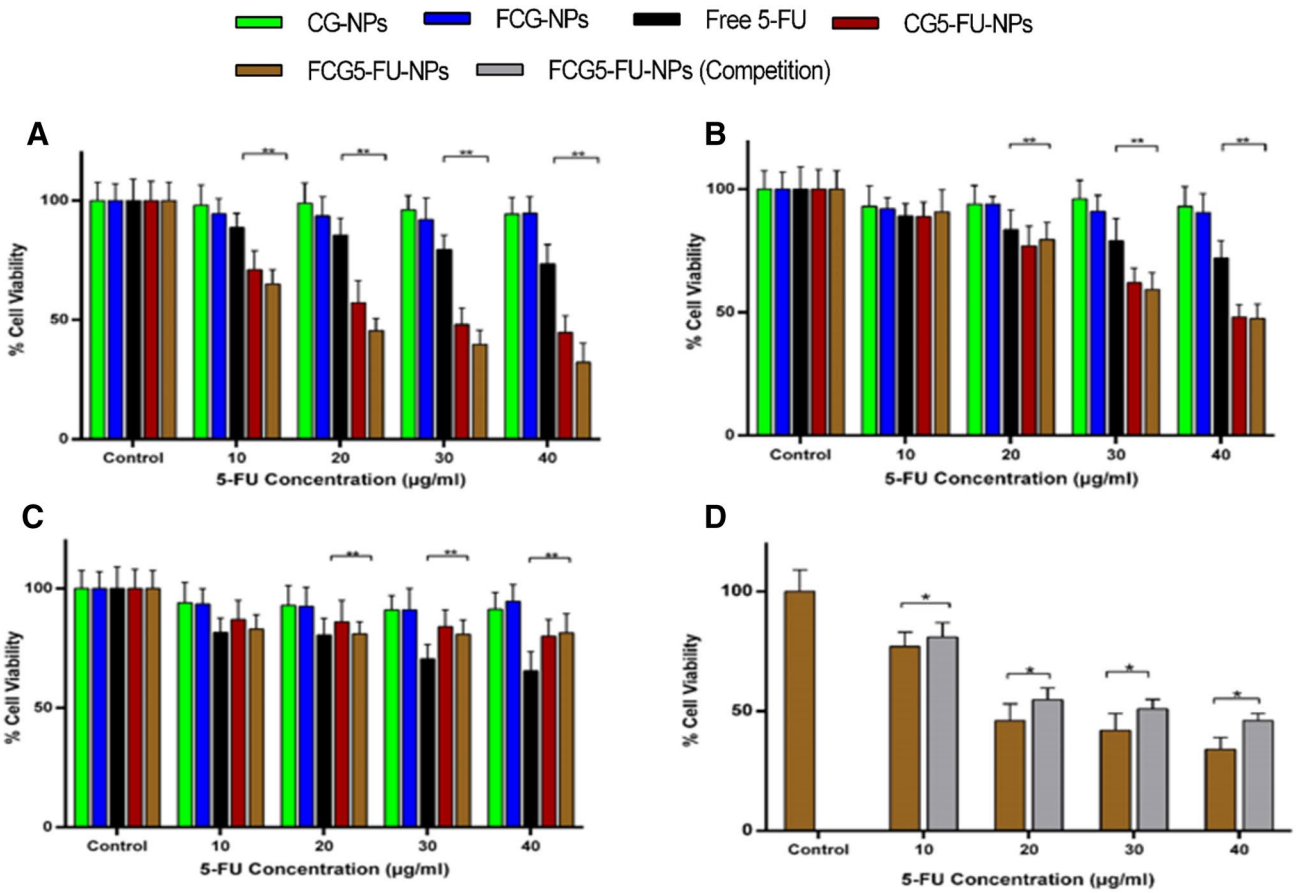

Fig. 6 MTT cell viability assay in vitro in human cell lines [A] MCF-7, [B] HepG-2, [C] HEK293 [D] MCF-7 (folate competition assay). Data are represented as means ± SD ($n = 3$), (**$p < 0.01$, *$p < 0.05$)

nucleolar chromatin condensation. Interestingly, MCF-7 cells treated with FCG5-FU-NPs showed the highest apoptotic index (0.56), with a significant decrease in the level of apoptosis observed following pre-treatment with folate in the competition assay. This suggests facilitated internalization of FCG5-FU-NPs by MCF-7 cells, attributable to the presence of the folate receptors on the cell surface. The high number of HEK293 cells which fluoresced green after

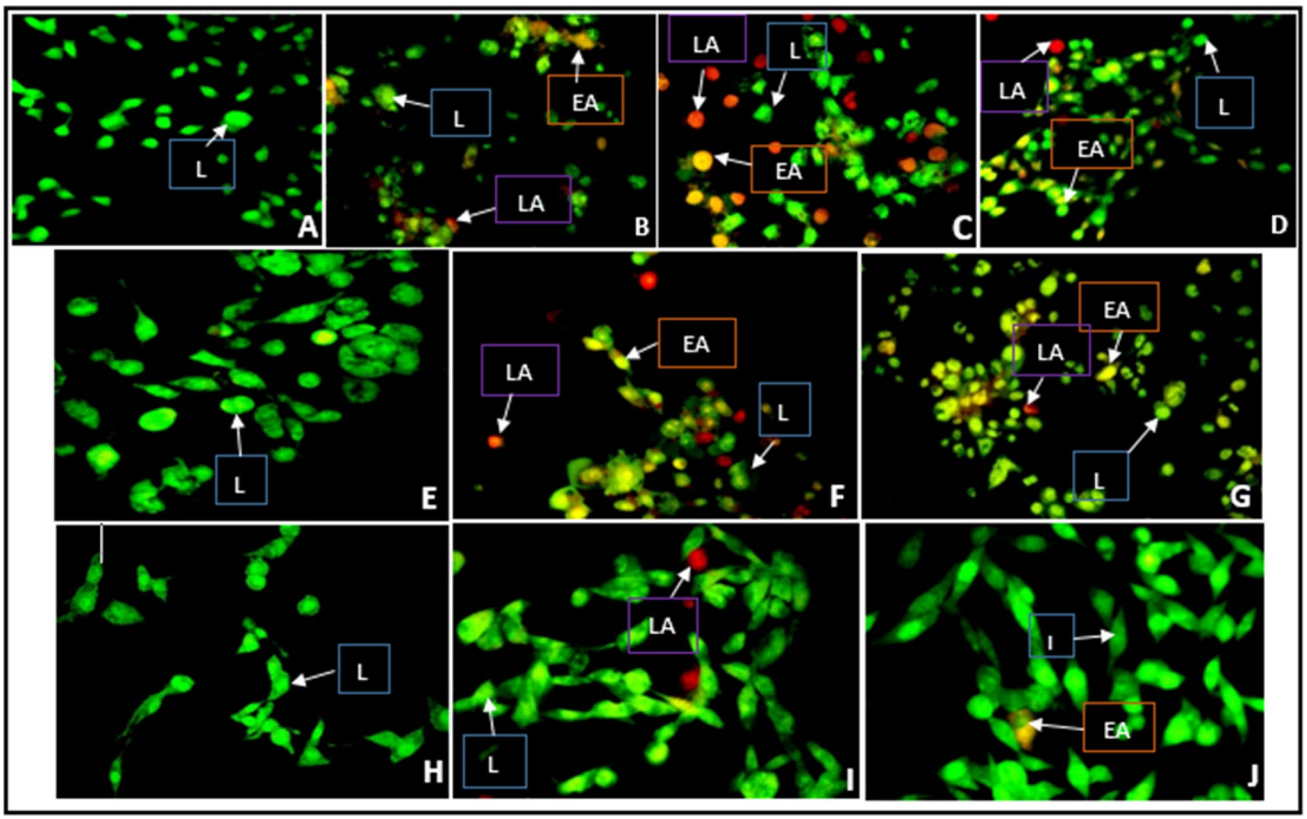

Fig. 7 Fluorescent images of AO/EB stained cells [A] MCF-7 control cells, [B] MCF-7 treated with CG5-FU-NPs, [C] MCF-7 treated FCG5-FU-NPs, [D] MCF-7 treated with FCG5-FU-NPs (competition assay), [E] HepG2 control cells, [F] HepG2 treated with CG5-FU-NPs, [G] HepG2 treated with FCG5-FU-NPs, [H] HEK293 control cells, [I] HEK293 treated with CG5-FU-NPs, [J] HEK293 treated with FCG5-FU-NPs. 20X magnification. *L* live cells, *EA* early apoptotic cells, *LA* late apoptotic cells

staining, demonstrated the relative non-toxic effects of all the drug-entrapped nanocomposites. Overall, these results were consistent with the findings of the MTT assay and further confirm the cell-specific delivery of CG5-FU-NPs and FCG5-FU-NPs, with the latter displaying enhanced delivery in FRα positive cancer cells.

Conclusion

In this present study, 5-FU was effectively encapsulated by the G-NPs, with chitosan and folate-chitosan serving as functionalizing and stabilizing agents. Also, the small-sized and spherical-shaped 5-FU encapsulated nanoconstructs, showed high colloidal stability and sustained pH dependent drug release. Further, drug release kinetics suggests zero-order mechanism of release at acidic and physiological pH conditions. In addition, better and selective anti-cancer effects were observed for the CG5-FU-NPs and FCG5-FU-NPs in the MCF-7 and HepG-2 cells, compared to the free drug, which may prove significant in the reduction of the eventual dosage regimen and subsequent off-target effects. Our study further revealed that FCG5-FU-NPs exerted higher anticancer activity than CG5-FU-NPs, in the folate receptor positive MCF-7 cells due to the presence of folate ligand, which actively targeted and enhanced the therapeutic efficacy of the nanocarrier by receptor mediation. Overall, these results confirm the potential of chitosan and folate-chitosan functionalized G-NPs as efficient delivery vehicles for 5-FU or similar chemotherapeutic agents. However, further studies would be done to further prove the in vivo suitability of these nanocarriers.

Acknowledgements The authors acknowledge the funding received from the National Research Foundation (NRF) [M Singh-Grant no: 81289], South Africa.

Compliance with ethical standards

Conflict of interest On behalf of all authors, the corresponding author states that there is no conflict of interest.

References

Akinyelu J, Singh M (2018) Chitosan stabilized gold-folate-poly (lactide-co-glycolide) nanoplexes facilitate efficient gene delivery in hepatic and breast cancer cells. J Nanosci Nanotechnol 18:4478–4486

Bertrand N, Wu J, Xu X, Kamaly N, Farokhzad OC (2014) Cancer nanotechnology: the impact of passive and active targeting in the era of modern cancer biology. Adv Drug Deliv Rev 66:2–25

Božanić DK, Trandafilović LV, Luyt AS, Djoković V (2010) 'Green'synthesis and optical properties of silver–chitosan complexes and nanocomposites. React Funct Polym 70:869–873

Carbinatto FM, de Castro AD, Evangelista RC, Cury BS (2014) Insights into the swelling process and drug release mechanisms from cross-linked pectin/high amylose starch matrices. Asian J Pharm Sci 9:27–34

Chakravarthi SS, Robinson DH (2011) Enhanced cellular association of paclitaxel delivered in chitosan-PLGA particles. Int J Pharm 409:111–120

Chen B, Le W, Wang Y, Li Z, Wang D, Ren L, Lin L, Cui S, Hu JJ, Hu Y, Yang P (2016) Targeting negative surface charges of cancer cells by multifunctional nanoprobes. Theranostics 11:1887

Danhier F, Feron O, Préat V (2010) To exploit the tumor microenvironment: passive and active tumor targeting of nanocarriers for anti-cancer drug delivery. J Control Release 148:135–146

Dash S, Murthy PN, Nath L, Chowdhury P (2010) Kinetic modeling on drug release from controlled drug delivery systems. Acta Pol Pharm 67:217–223

Dauthal P, Mukhopadhyay M (2016) Noble metal nanoparticles: plant-mediated synthesis, mechanistic aspects of synthesis, and applications. Ind Eng Chem Res 55:9557–9577

Devendiran RM et al (2016) Green synthesis of folic acid-conjugated gold nanoparticles with pectin as reducing/stabilizing agent for cancer theranostics. RSC Adv 6:29757–29768

Dhar S, Reddy EM, Shiras A, Pokharkar V, Prasad BE (2008) Natural gum reduced/stabilized gold nanoparticles for drug delivery formulations chemistry-A. Eur J 14:10244–10250

Dhas NL, Ige PP, Kudarha RR (2015) Design, optimization and in-vitro study of folic acid conjugated-chitosan functionalized PLGA nanoparticle for delivery of bicalutamide in prostate cancer. Powder Technol 283:234–245

Haiss W, Thanh NT, Aveyard J, Fernig DG (2007) Determination of size and concentration of gold nanoparticles from UV–Vis. spectra. Anal Chem 79:4215–4221

Ismail ST, Al-Kotaji MM, Khayrallah AA (2017) Formulation and evaluation of nystatin microparticles as a sustained release system. Iraqi J Pharm Sci 24:1–10

Kang B-S et al (2017) Enhancing the in vitro anticancer activity of albendazole incorporated into chitosan-coated. PLGA Nanoparticles Carbohydr Polym 159:39–47

Kuksal A, Tiwary AK, Jain NK, Jain S (2006) Formulation and in vitro, in vivo evaluation of extended-release matrix tablet of zidovudine: influence of combination of hydrophilic and hydrophobic matrix formers. AAPS PharmSciTech 7:E1–E9

Lazarus GG, Singh M (2016) Cationic modified gold nanoparticles show enhanced gene delivery in vitro. Nanotechnol Rev 5:425–434

Lee SJ, Min HS, Ku SH, Son S, Kwon IC, Kim SH, Kim K (2014) Tumor-targeting glycol chitosan nanoparticles as a platform delivery carrier in cancer diagnosis therapy. Nanomedicine 9:1697–1713

Madhusudhan A, Reddy GB, Venkatesham M, Veerabhadram G, Kumar DA, Natarajan S, Yang MY, Hu A, Singh SS (2014) Efficient pH dependent drug delivery to target cancer cells by gold nanoparticles capped with carboxymethyl chitosan. Int J Mol Sci 15:8216–8234

Maiyo F, Moodley R, Singh M (2016) Cytotoxicity, antioxidant and apoptosis studies of quercetin-3-O glucoside and 4-(β-D-glucopyranosyl-1→ 4-α-L-rhamnopyranosyloxy)-benzyl isothiocyanate from Moringa oleifera. Anticancer Agents Med Chem 16:648–656

Maney V, Singh M (2017) An in vitro assessment of chitosan/bimetallic PtAu nanocomposites as delivery vehicles for doxorubicin. Nanomedicine 12:2625–2640

Nivethaa E, Dhanavel S, Narayanan V, Vasu CA, Stephen A (2015) An in vitro cytotoxicity study of 5-fluorouracil encapsulated chitosan/gold nanocomposites towards MCF-7 cells. RSC Adv 5:1024–1032

Ofokansi KC, Adikwu MU, Okore VC (2007) Preparation and evaluation of mucin-gelatin mucoadhesive microspheres for rectal delivery of ceftriaxone sodium. Drug Develop Ind Pharm 33:691–700

Parker WB, Cheng YC (1990) Metabolism and mechanism of action of 5-fluorouracil. Pharmacol Ther 48:381–395

Pauliukaite R, Ghica ME, Fatibello-Filho O, Brett CM (2010) Electrochemical impedance studies of chitosan-modified electrodes for application in electrochemical sensors and biosensors. Electrochim Acta 55:6239–6247

Ritger PL, Peppas NA (1987) A simple equation for description of solute release II. Fickian and anomalous release from swellable devices. J Control Release 5:37–42

Safwat MA, Soliman GM, Sayed D, Attia MA (2016) Gold nanoparticles enhance 5-fluorouracil anticancer efficacy against colorectal cancer cells. Int J Pharm 513:648–658

Salar RK, Kumar N (2016) Synthesis and characterization of vincristine loaded folic acid–chitosan conjugated nanoparticles. Res-Effic Technol 2:199–214

Samadian H, Hosseini-Nami S, Kamrava SK, Ghaznavi H, Shakeri-Zadeh A (2016) Folate-conjugated gold nanoparticle as a new nanoplatform for targeted cancer therapy. J Cancer Res Clin Oncol 142:2217–2229

Singh J, Roychoudhury A, Srivastava M, Solanki PR, Lee DW, Lee SH, Malhotra B (2014) A dual enzyme functionalized nanostructured thulium oxide based interface for biomedical application. Nanoscale 6:1195–1208

Song H, Su C, Cui W, Zhu B, Liu L, Chen Z, Zhao L (2013) Folic acid-chitosan conjugated nanoparticles for improving tumor-targeted drug delivery. BioMed Res Int 2013:723158

Sood A, Panchagnula R (1998) Drug release evaluation of diltiazem CR preparations International. J Pharm 175:95–107

Steichen SD, Caldorera-Moore M, Peppas NA (2013) A review of current nanoparticle and targeting moieties for the delivery of cancer therapeutics European. J Pharm Sci 48:416–427

Tan Q, Chu Y, Bie M, Wang Z, Xu X (2017) Preparation and investigation of amphiphilic block copolymers/fullerene nanocomposites as nanocarriers for Hydrophobic. Drug Mater 10:92

Turkevich J, Stevenson PC, Hillier J (1951) A study of the nucleation and growth processes in the synthesis of colloidal gold. Discuss Faraday Soc 11:55–75

Udofot O, Affram K, Bridg'ette Israel EA (2015) Cytotoxicity of 5-fluorouracil-loaded pH-sensitive liposomal nanoparticles in colorectal cancer cell lines. Integr Cancer Sci Ther 2:245

Uhrich KE, Cannizzaro SM, Langer RS, Shakesheff KM (1999) Polymeric systems for controlled drug release. Chem Rev 99:3181–3198

Upadhyaya L, Singh J, Agarwal V, Pandey A, Verma SP, Das P, Tewari R (2015) Efficient water soluble nanostructured ZnO grafted O-carboxymethyl chitosan/curcumin-nanocomposite for cancer therapy. Process Biochem 50:678–688

Venkatpurwar V, Shiras A, Pokharkar V (2011) Porphyran capped gold nanoparticles as a novel carrier for delivery of anticancer drug: in vitro cytotoxicity study. Int J Pharm 409:314–320

Wang C, Shaw LL (2014) On synthesis of Fe_2SiO_4/SiO_2 and Fe_2O_3/SiO_2 composites through sol–gel and solid state reactions. J Sol-gel Sci Technol 72:602–614

Yang C-L, Chen J-P, Wei K-C, Chen J-Y, Huang C-W, Liao Z-X (2017) Release of doxorubicin by a folate-grafted, chitosan-coated magnetic nanoparticle. Nanomaterials 7:85

Yassin AEB, Anwer MK, Mowafy HA, El-Bagory IM, Bayomi MA, Alsarra IA (2010) Optimization of 5-flurouracil solid-lipid nanoparticles: a preliminary study to treat colon cancer. Int J Med Sci 7:398